

# DEMONSTRATION OF THE EXISTENCE OF THERMAL SURFACE ENERGY AND ITS IMPACTS.

*A. Titov, PhD*

Physics Department, Yeditepe University, Istanbul, Turkey

*I. Malinovsky PhD*

National Metrology Institute, INMETRO, Rio de Janeiro, Brazil

---

## Abstract

Using variation principle, we have demonstrated experimentally, for the first time, the existence of the thermal surface energy (TSE), resulting from the oriented motion of charged particles inside a material artefact and the energy of the guided electromagnetic (EM) field, which always accompanies the irregular motion of charged particles. The TSE arises gradually as an evolution process of hysteresis type as a result of interaction of the external EM field, characterized by a mean nonzero value of the Poynting vector, with an ensemble of charged particles of material artefact. It has been demonstrated experimentally that the principle of superposition of the external EM fields is not valid in case of TSE, and an artefact is shown to be in a continuous thermal evolution process, which has no symmetry in space and is irreversible in time, clearly confirming the preceding theoretical results of (Dicke 1954). Such process can be called as thermal synthesis. It is shown that the number of influence parameters, necessary for the description of the thermal evolution process is always huge, thus presenting an experimental confirmation of the fundamental theoretical observation of (Stroud et al. 1972, p.1096). We have shown experimentally for the first time that in a homogeneous material a heat source induces a larger flux of energy in a specified direction, if the energy flux in that direction has been created before by an auxiliary heat source. A deep agreement of our studies with Ancient Indian and Greek Philosophies, as well as with the classical German dialectics is outlined.

---

**Keywords:** Surface energy, thermodynamic temperature, hysteresis, synthesis

## 1. Introduction

This communication we want to start with reminding of the theoretical prediction (Einstein 1905, p.550):“classical thermodynamics can no longer be looked upon as applicable with precision...For the calculation of the free energy, the energy and the entropy of the boundary surface should also be considered”. Important advancement of these ideas one can find in a popular University text-book (Sivukhin 2008a, p.55), where the thermal surface energy (TSE) is defined as the energy of boundary zones, located between the macroscopic parts of the system (sub-systems), in which the quasi-equilibrium thermal conditions are realized. It is stated (Sivukhin 2008a) that the TSE is proportional to the area of contact between the two sub-systems, and that *the internal energy of the system can be considered as additive, only when the value of the TSE can be regarded as negligible*. It is clear that if the TSE were observed experimentally, the concept of thermodynamic temperature (Sivukhin 2008b), the only one which exists in theoretical Physics, should be somehow modified: it should be, at least, in agreement with the notion of “temperature”, which is traditionally used in the J. Fourier thermal conduction theory (Sivukhin 2008c) and which definitely refers to thermal non-equilibrium conditions. Meanwhile, in accordance with (Einstein 1903, p.170), thermodynamics can be applied only to isolated systems, and when all the transients in the system have finished.

The studies, presented here, are in agreement with the main features of the above mentioned theoretical predictions, but the experiment has discovered the effects of paramount importance, which the indicated theoretical considerations do not contain. By our experiments, we have demonstrated the existence of the TSE with a signal-to-noise ratio of more than 1000. The TSE presents the variations of the energy, which can be registered by thermometers and which are associated with the oriented propagation of energy and momentum in the field-particle system under non-equilibrium thermal conditions. *The fundamental features of the TSE are the lack of symmetry in space and the irreversible character of its evolution in time*. In this respect, the TSE is similar to the hysteresis effects in ferromagnetic (Sivukhin 2008d) and ferroelectric materials (Sivukhin 2008e). And indeed, the hysteresis loop of the TSE, observed in steel and presented in this paper, resembles the hysteresis loop of a hard ferromagnetic material under very long exposure to a strong magnetic field. It is shown that, as a result of the nonlinearities, which are always present in any thermal system, the principle of superposition of the electro-magnetic (EM) fields in case of the TSE is not valid, and two heat sources are interacting continuously in time with each other through the TSE (as a result of the emission of the EM radiation). *As the number of macroscopic parameters, necessary for the description of TSE is always huge and the internal energy*

of the system has to include TSE (as a part of thermal energy susceptible by thermometers), the *internal energy and temperature cannot be considered as functions of state* (Sivukhin 2008a). Thus, the extension of the concept of temperature (as a measure of the internal energy) beyond the approximation of the thermal equilibrium conditions, is becoming inevitable.

Our experiments have also shown that as a result of violation of the superposition principle, the presence of an additional heat source modifies the hysteresis loop of the TSE, produced by the modulated energy source. In the presence of the time irreversible external heat source (for example, Sun radiation on the Earth's surface), the thermal hysteresis loop for the continuous sweep in time converts into the non-periodic spiral, in which each cycle has slightly different form and magnitude from the previous ones. It is found that the appearance of the TSE is accompanied by the creation of the new properties of the artifact (deformations and stresses in the lattice, mass transfer of free electrons, appearance of the wave-momentum density and its current densities in the artifact material) that do not exist at all under the thermal equilibrium. As the thermal evolution process is irreversible in time, has no symmetry in space, as it is specific for each particular point of the artifact and represents the variation of the basic physical parameters of the system under the varying external conditions, the most appropriate way to describe it is to use the *concept of synthesis*. Here, we are to remind that this concept was first introduced by the German philosopher H. M. Chalybäus, then it was elaborated on by the German philosopher J. G. Fichte, and later it was incorporated into dialectics together with the famous triad (thesis-antithesis-synthesis). Nowadays, in a quite similar meaning, it is commonly used in chemistry.

## **2. Experiment.**

The presented studies are based on the variation principle - one of the most general and powerful principles in experimental physics. We have used a recently developed (Titov & Malinovsky 2005) multi-channel synchronous detection technique (MSDT), which presents some modification of the famous R. Dicke's method of synchronous detection. The specific feature of MSDT is that the modulation of the heat input to the system is realized through thermometer in one of the channels, and the detection is realized by several temperature sensors of the other channels, which are located at different positions relative to the modulation source (Titov et al. 2005.). In this case, the temperature information from the modulation channel can be used to find the synchronous temperature differences between the different points of the system, and, consequently, the propagation of the thermal signals can be precisely characterized both in time and in space. The second distinguishing feature of MSDT is the use of long modulation periods (Titov & Malinovsky 2011) (several hours, in typical cases), so that the necessary

averaging procedures can be performed independently within the parts of each modulation cycle. Quite long modulation periods give an additional opportunity to use high-precision bridges, and to achieve with their help the resolution of temperature measurements of about  $1\mu\text{K}$  at room temperatures (Titov, Malinovsky & Masssone 2001, p. 37; Titov et al. 2005, p. 587904-5) that corresponds to the value of  $3 \times 10^{-9}$  in relative units. So, if we realize the modulation amplitude of  $\sim 20\text{mK}$  inside an artifact, and the artifact changes significantly its properties at  $2000\text{K}$ , then the modulation signal of this level will produce a huge non-linearity in the thermal system, which can be in detail studied using MSDT.

A schematic outline of our experimental set-up and an example of unprocessed results of the measurements, performed on a homogeneous steel artifact, are presented in Fig.1. A steel (or tungsten carbide) gauge block (GB), with dimensions  $9 \times 35 \times 100$  mm, is located horizontally on three small-radius, polished spheres inside a closed Dewar. The Dewar is kept in a temperature controlled room, where typical temperature variations can be characterized by a standard deviation  $\sigma$  of  $\sim 50\text{mK}$ . Two thermistors R6 and R3, belonging to channels 1 and 2 respectively, are installed on the surface of the GB in copper adapters, whose axes are parallel to the gauging surfaces. A 100-Ohm platinum resistance thermometer (PRT), also in a copper adapter, is located parallel to thermistors and at equal distances from their adapters. The PRT is connected to MI-bridge T615 (Canada), in which the current  $I$  is changed by step from 1 to 5mA (Fig.1). The period of the modulation cycle is  $\sim 148$  minutes, and for 37 minutes the current  $I$  is 5mA, and for the rest of the modulation cycle it is held at 1mA level.

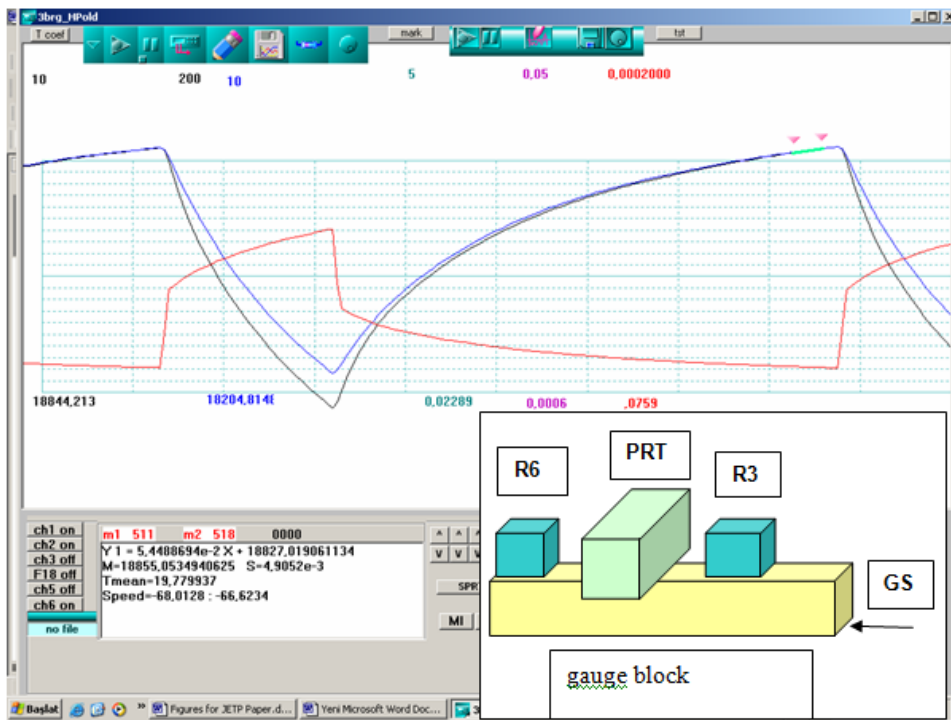


**Fig.1.** Simultaneous records of the resistance variations of the platinum resistance thermometer (PRT) and of two thermistors R6 and R3, located symmetrically relative to the PRT on the surface of the gauge block (as shown in the insert). During the current modulation cycle in the PRT, its current for  $\frac{1}{4}$  of the modulation period is kept at the level of 5mA and  $\frac{3}{4}$  of the period is kept at 1mA. The sensitivities of the thermistors are equal. The location of one of the gauging surfaces, characterized by roughness variations and deviations from flatness at the nm scale, is shown by the arrow. (See text for other details).

In Fig.1, the PRT measurements correspond to the record with faster transients. Two other records show the variations of resistances of the two temperature calibrated thermistors R6 and R3, which have negative temperature coefficients. The thermistors are connected to high-precision multi-meters HP-35a, and are calibrated together with the multi-meters, using the procedure described in (Titov et al. 2005). Both thermistors have, practically, equal sensitivities, and as the temperature variations in Fig.1 for both channels do not reach 35mK, the difference between the resistance variations for both channels in Fig.1 is not distinguishable at the resolution level of the presented plot from the difference between the corresponding temperature variations in the channels. The accurate mean values of the temperatures and of the temperature rates, calculated on the basis of the experimental calibration equation, for the desired time interval (indicated by two triangular cursors of the program) for each channel can be obtained in a

special window of the program (Fig.1). For example, from the presented plots in Fig.1 it follows that the temperature difference between the channels  $T[1,2]$  for the last 25 minutes of the first cycle (shown in Fig.1) was  $465.6\mu\text{K}$ . The standard deviation  $\sigma$  for a single measurement point (with 5min. averaging time) was found to be  $3.3\mu\text{K}$ . For the last 25 minutes of the next cycle, the value of  $T[1,2]$  was  $469.5\mu\text{K}$ , with a  $\sigma$ -value of  $2.3\mu\text{K}$ . The temperature drift of the quantity  $T[1,2]$  of less than  $4\mu\text{K}$  for more than 2 hours gives a clear indication that these points, corresponding to the PRT current value of  $1\text{mA}$ , define quite accurately the reference function at  $I=1\text{mA}$  (which can be presented, for example, by a linear regression equation for the presented plot). And after that, the *induced temperature variations  $\Delta T[1,2]$*  (at  $I=5\text{mA}$ ) *can be determined very precisely relative to the determined reference function.*

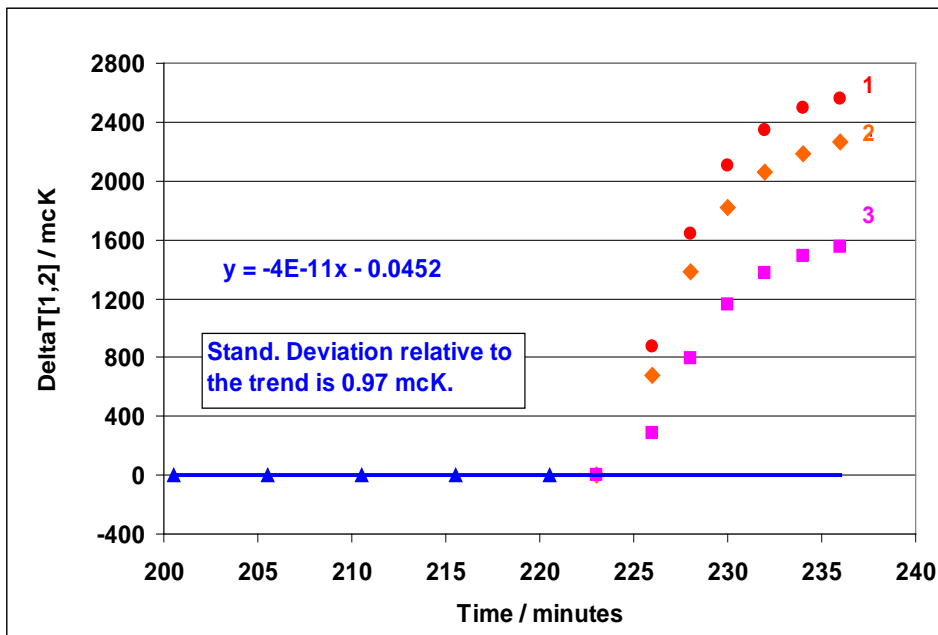


**Fig.2a.** Dependences on time of the thermal surface energy (TSE), characterized by the quantity  $\Delta T[1,2]$  and measured in  $\mu\text{K}$  on the axis of the  $R_0$  separations  $L$  of thermistor from the gauging surface: The corresponding dependences for  $L$ -values of  $4.5\text{mm}$ ,  $9\text{mm}$  and  $13.5\text{mm}$  are marked by dots, rhombi and squares, respectively.

The result of paramount importance, which can be clearly detected even from a couple of cycles of Fig.1, is that the *variations of the thermal energies  $\Delta T[1,2]$* , produced by the increased level of the power dissipated in the PRT, are not equal at the equal distances from a heat source in a homogeneous artifact, so that the arising distribution of thermal energy on the artifact surface has no spatial symmetry relative to the heat source. The thermometer, which is closer to the boundary (gauging surface), detects

always a higher level of the temperature variation during the heating period of the modulation cycle at  $I=5\text{mA}$ . And this is a demonstration of the existence of the *thermal surface energy*. Indeed, on one hand, the record is performed by thermometers and, consequently, this is a “thermal energy”. And on the other hand, as it is clearly demonstrated by the plot of Fig.2a, the TSE value drops in a fast way with the increase of the distance from the boundary of the artifact. So, this type of energy should be, naturally, called as “surface energy”. Starting with Fig.2, in the majority of the experiments, the dependence of the reference values on time was obtained by 6-th order polynomial fit to all of the last 25-minute points, obtained for the cooling periods of the modulation cycles at  $I=1\text{mA}$ . The total duration of the experimental record was usually about 16 hours. Naturally, as a result of the averaging procedure over several modulation cycles, the uncertainty of the measurements is further improved. For example, the standard deviation  $\sigma$  of a single reference point in Fig.2a is  $0.97\mu\text{K}$ . Meanwhile, the TSE magnitude for one of the dependences in Fig.2a (shown with dots) for the time interval 13 minutes after the increase of the PRT modulation current is more than  $2500\mu\text{K}$ , and the signal still continues to increase further. So, our measurement system detects with the huge signal-to-noise ratio that for the sensor R6, located closer to the boundary, the temperature variations,  $\Delta T[1]$ , induced by the PRT current of  $5\text{mA}$ , for all time intervals (used in our experiments) are larger than the corresponding variations,  $\Delta T[2]$ , recorded by the sensor R3. In Fig.2a, the resulting difference in temperature variations is denoted by  $\Delta T[1,2]$ , and the corresponding function  $\Delta T[1,2]$  on time (under the experimental conditions of Fig.1) is presented by dependence 1 (dots). Here, one of the surfaces of the R6 adapter was located in the plane of the gauging surface of the artifact, so that the distance  $L$  of the axis of the thermistor R6 relative to the gauging surface was  $4.5\text{mm}$ . In this case, for the measurements, performed 13 minutes after the increase of the PRT current to  $5\text{mA}$ , the *induced temperature difference*  $\Delta T[1,2]$  was  $2563\mu\text{K}$ . Here, it is worthy of note that the total spread of the obtained values of  $\Delta T[1,2]$  for individual cycles of the series was within  $\pm 1.5\mu\text{K}$  for that time interval. The experimental uncertainties are not shown on the plot, as they are significantly smaller than the size of the symbols, used to denote the experimental points.

Then, all the thermometers were shifted together from the gauging surface in a parallel way, so that all the separations between them were kept constant. The corresponding decrease of the quantity  $\Delta T[1,2]$  with the increase of the distance from the boundary is demonstrated by two other plots in Fig.2a. Here, the dependences 2 and 3 of  $\Delta T[1,2]$  on the time elapsed (after the increase of the PRT current) are shown for the distances  $L=9\text{mm}$  and  $L=13.5\text{mm}$  by rhombs and squares, respectively. It is also worth noting here, that when the system of thermometers as a whole was shifted to

the opposite gauging of the block, so that the axis of the thermistor R3 is located at the distance 4.5mm from the nearest gauging surface, the quantity  $\Delta T[1,2]$  changes the sign, but the absolute values of the dependence of  $\Delta T[1,2]$  on time, within the experimental errors, coincide with the corresponding values of the dependence 1. The experimental dependence of the quantity  $\Delta T[1,2]$  on the distance of the heat source X relative to the center of the surface of the block is shown in Fig.2b by a solid line. Here, the values of the quantity  $\Delta T[1,2]$  as a function of the PRT displacement X are presented for the fixed time interval, which is equal to 13 minutes after the increase of the PRT current. The distances between the axis of the PRT and the axes of both thermistors were equal to 19mm in this experiment. The maximum value of the PRT distance from the center of the surface  $X=26.5\text{mm}$  in Fig.2b corresponds to the minimum distance  $L=4.5\text{mm}$  of the thermistor R6 from the gauging surface in Fig.2a.

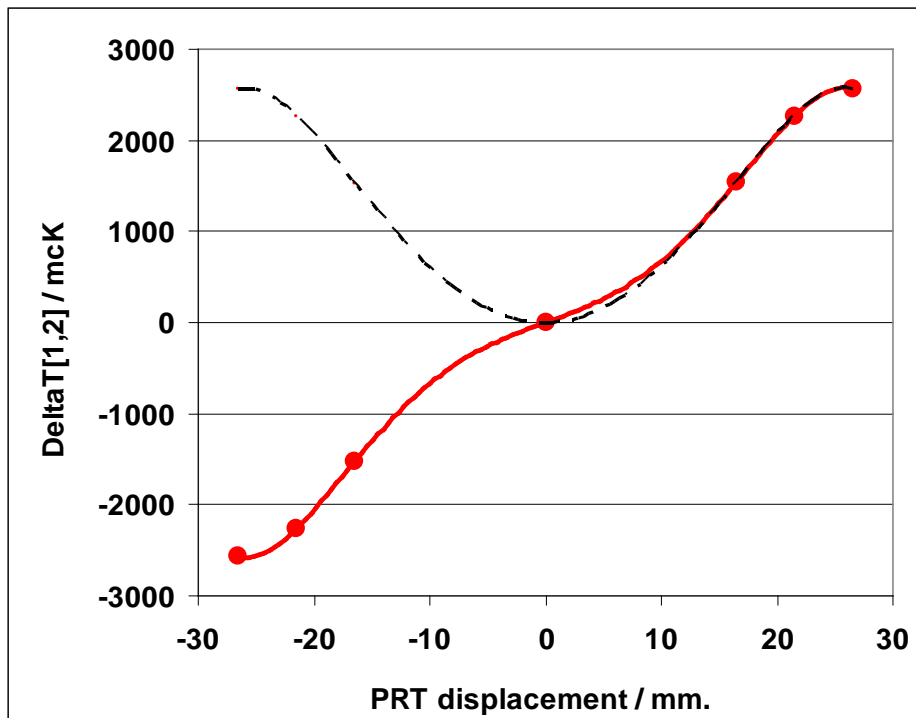


**Fig.2b.**The dependence of the quantity  $\Delta T[1,2]$ , measured in (solid line) and the dependence of its absolute value (dashed line) as functions of the displacement of the PRT axis from the center of the block surface.

The absolute value of the quantity  $\Delta T[1,2]$  as a function of the displacement X is shown in Fig.2b as a dashed line. Here again, all of the data-points correspond to the heating period of the modulation cycle for the time interval of 13 minutes. From this plot the surface origin of the effect is



demonstrated quite clearly. The function  $|\Delta T[1,2]|$  acquires its maximum values when one of the surfaces of the adapters of the thermistors R6 or R3 coincides with the gauging surface of the block (see inset of Fig.1). For the symmetric location of the PRT on the block surface ( $X=0$ ) the absolute value of the quantity  $\Delta T[1,2]$  is, naturally, equal to zero. It should be taken into consideration that for all displacements  $X$ , the *mean value of  $\Delta T[1,2]$  for the reference points (at  $I=1mA$ ) is also automatically equal to zero* as a result of the adopted measurement method, based on the variation principle.

In contrast to the modulus, the *quantity  $\Delta T[1,2]$  carries the information about the direction*. As our measurement system is susceptible to the temperature variations only in one direction (i.e. in the direction of the longest side of the rectangular block), the direction of the excessive energy propagation can be adequately described by the sign: plus or minus. For example, the positive value of the quantity  $\Delta T[1,2]$  corresponds to the excessive flux of thermal energy during the heating period of the modulation cycle to the unit volumes inside the block in the vicinity of the thermistor of channel 1, relative to the corresponding unit volumes in the vicinity of the thermistor of channel 2. So, the TSE is characterized by the vector quantity  $\Delta T[1,2]$ , which is shown in the text in a bold font. The vector character of the quantity  $\Delta T[1,2]$  also follows from the plot of Fig.2b, where the presented function is anti-symmetric relative to the PRT displacement  $X$ . Here, we can conclude that the existence of TSE, characterized by the vector quantity  $\Delta T[1,2]$ , has been demonstrated with the signal-to-noise ratio of more than 1000 under different experimental conditions.

In (Titov & Malinovsky 2005) it has been shown experimentally that when finding the relation under non-equilibrium conditions between the two thermometers, located inside a homogeneous material, the velocity-error correction terms has to be included. For example, in the simplest case of a one-dimensional field distribution and for the achieved steady-state, “asymptotic” process, the velocity-error correction is given by the product  $V\tau$  (Titov & Malinovsky 2005, p. 587902-03). Here, the thermal velocity  $V$  should be considered as a vector quantity, whose value is positive for the input of thermal energy to the system, and is negative for the loss of the energy by the system; and  $\tau$  is the effective time, depending on the propagation time of the heat signal between the positions of the thermometers. The vector type of this correction gives an indication to the “oriented force action” (when borrowing the terminology of A. Einstein (1917)), and this vector is also an indication to the thermal surface energy of the present studies.

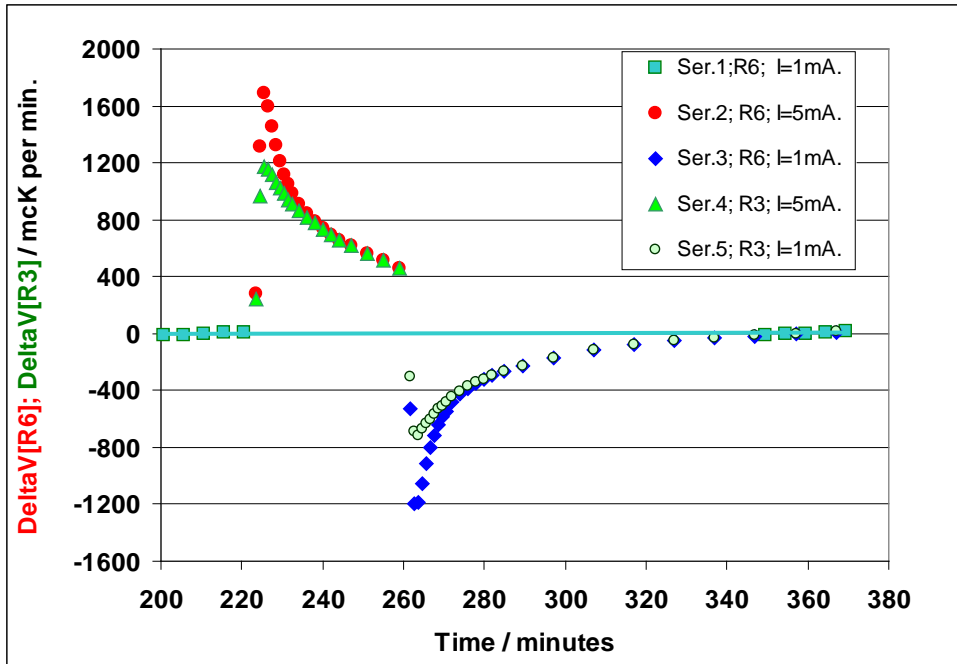


**Fig.3a.** Variations in time of the temperature rates (in  $\square K / \text{min.}$ ) of the thermistor R6,  $\Delta V[R6]$ , (dots and rhombi) and of the thermistor R3,  $\Delta V[R3]$ , (triangles and circles) for  $I=5\text{mA}$  (dots and triangles) and for  $I=1\text{mA}$  (rhombi and circles). (See text for other details).

So, to clarify further the origin of the TSE, we studied experimentally the *variations of the thermal velocities* (Fig.3a), which were induced by 5mA current and recorded simultaneously by both thermistors. The temperature velocities  $V[R6]$  and  $V[R3]$  can be measured by the PC program (Fig.1) by selecting the desired time interval by two cursers. The variations  $\Delta V[R6]$  and  $\Delta V[R3]$  (induced by the current variations) were determined using the MSDT procedure, similar to the one used in the studies of temperature variations. The variations  $\Delta V[R6]$  and  $\Delta V[R3]$ , observed in the steel GB during one modulation cycle under the experimental conditions, corresponding to the dependence 1 in Fig.2a, are shown in Fig.3a. It follows from the comparison of records of two channels, that the thermistor R6, which is located closer to the gauging surface, detects much larger variations of the thermal rates during a relatively short period of time after the each change of the PRT current (in the process of the realization of the modulation cycle) in comparison with the thermistor R3. To observe clearly the net effect, in Fig.3b we present the difference between the induced thermal velocities  $\Delta V[1,2]$ , recorded synchronously by the two channels under the experimental conditions of Fig.1. From the comparison of the dependences of Figs. 3a and 3b, we can infer that the thermistor R6, which is closer to the gauging surface, records two processes, characterized by two

different time scales. The background is the process, which is characterized by the larger time scale and which is very close to the energy propagation process, recorded by the thermistor R3. This follows from the comparison of both dependencies in Fig.3a for the time intervals, 18-20 minutes after the switch of the current in the PRT, both for the heating and for the cooling periods of the modulation cycle. For these parts of processes, the energy inputs and losses per unit time are the same for the elementary volumes of the GB, located under the adapters of the thermistors of both channels. Thus, these parts are symmetric in space to very high level of precision. They can be studied in detail during the GB cooling process, which lasts ~2 hours. We can assume that these slower processes are related to the diffusion process, which forms the basis of the Fourier thermal conductivity theory (Sivukhin 2008c). On this slower process, the faster process in R6 is superimposed. As it follows from Fig.3b, it is observed only at the initial stages of the heat transfer after the square-wave current changes, both positive and negative. This process is related to the vector quantity  $\Delta V[1,2]$ , which has a spatial anti-symmetric dependence similar (but not equal) to the dependence of the quantity  $\Delta T[1,2]$ , presented in Fig.2b. As it will be shown below, the quantity  $\Delta V[1,2]$  describes (by its sign and value) the difference in the energy fluxes through the boundary surfaces to the corresponding elementary volumes inside the artifact, located under the temperature sensors of the channels 1 and 2. Meanwhile, the quantity  $\Delta T[1,2]$  characterizes the value and the sign of the temperature (or energy) difference between the corresponding unit volumes of the artifact, accumulated up to the specified time moment. It follows from the experiment that the characteristic length for the quantity  $\Delta V[1,2]$  is smaller than the one of the quantity  $\Delta T[1,2]$ . But here, it is important to emphasize that the anti-symmetric spatial dependence of the quantity  $\Delta V[1,2]$  ruins the symmetry in space of the total energy transfer process in the vicinity of the gauging surface, for which the fluxes of energy through the boundaries of the elementary volumes are characterized by the time dependences of the quantities  $\Delta V[R6]$  and  $\Delta V[R3]$  in Fig.3a.

As  $\Delta V[1,2]$  is a vector quantity, it is shown in the text by a bold font. It describes, for example, the build up of the surface thermal energy (TSE), resulting from the additional energy fluxes to the elementary volumes in the vicinity of the R6 sensor at the initial stages of the heating period (at  $I=5\text{mA}$ ) of the modulation cycle. The plots of Figs.3a and 3b demonstrate also an almost symmetrical negative energy fluxes, resulting in the decrease of the surface energy, at the initial stages of the cooling period of the cycle at  $I=1\text{mA}$ . As in our set-up, the adapters of the thermistors cover the whole width of the GB surface, and the height of the GB (9mm) is much smaller than its length, our system records the difference in thermal velocities along the axis of symmetry of the GB, parallel to its longer side.

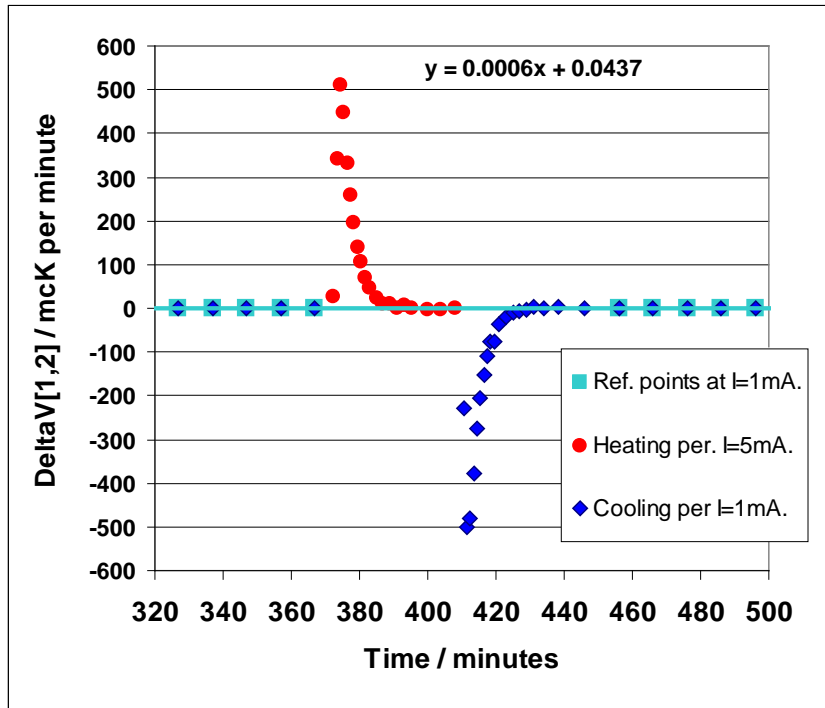


**Fig.3b.** Variations in time of the difference between induced temperature velocities (in  $\mu\text{K} / \text{min.}$ ) of the channels 1 and 2,  $\Delta V[1,2]$ , observed during the heating period ( $I=5\text{mA}$ ) of the modulation cycle (dots) and during the cooling period ( $I=1\text{mA}$ ) of the modulation cycle (rhombi) and measured relative to the reference points, shown as squares.

The results of the next experiment, which clarifies further the origin of TSE, are shown in Fig.4. Here, with vanishingly small uncertainty it is demonstrated that the magnitude of TSE is linearly related to the power, delivered to the GB by PRT. The presented plots correspond to the values of the temperature differences  $\Delta T[1,2]$ , arising in the channels (1 and 2) in the steel GB 13 minutes after the increase of the current in the PRT under the experimental conditions, corresponding to the dependences 1 and 3 in Fig.2. The presented power levels are calculated for the upper current values of 3mA and 5mA, which were realized in the modulation cycles of two independent experiments. To demonstrate the reliability of the measurement procedure, the plots are obtained for two different separations  $L$  of the center of the thermistor  $R[6]$  from the nearest gauging surface: 4.5mm (dots) and 13.5mm (squares), respectively. For the dependence 1, the maximum deviation for the three points (including the origin) is  $0.24\mu\text{K}$ . We are to note here that the similar plots have been obtained for the maximum value of the quantity  $\Delta V[1,2]$  versus power delivered to the GB. But these plots appear indistinguishable (within the graphical resolution) with the plots of Fig.4, and, consequently, only one plot is presented.

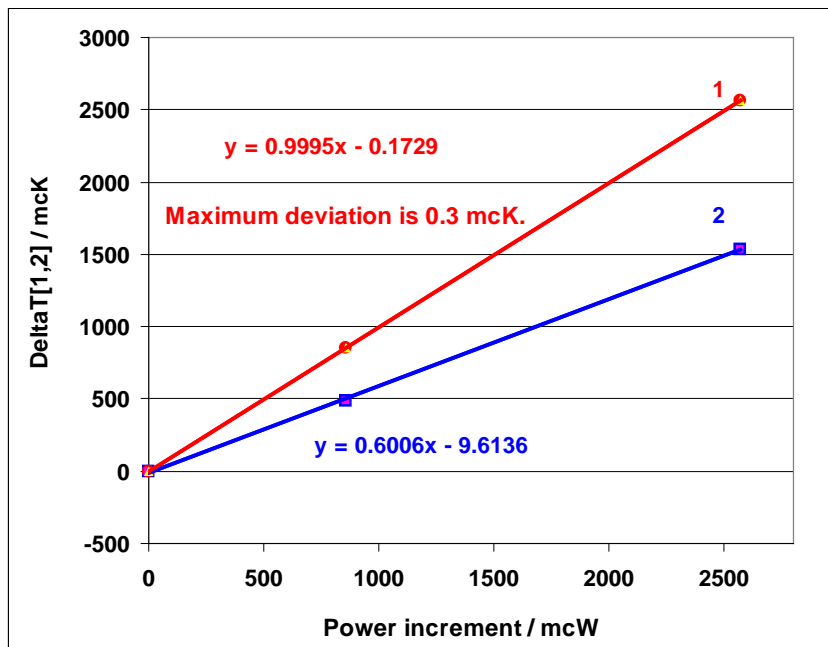


**Fig.4.** The dependences of the quantity  $\Delta T[1,2]$  (in (measured in surface of  $L=4.5\text{mm}$  (dots) and  $L=13.5\text{mm}$  (squares). (See text for other details).

$\square$ K) on the PRT in  
 $\square$ W), obtained for

After establishing the linear relation between the TSE and the absorbed power in the GB, the origin of the TSE is revealed further: the only macroscopic vector quantity, representing the external influence parameter in our experiment, is the Poynting vector of the absorbed EM radiation, which is generated by the DC current source in the process of acceleration of free electrons in the PRT (Griffiths 1999, p. 460). When recalling the fundamental J. C. Maxwell’s conclusion that the power of the EM field, absorbed in or reflected from a material object, results in the oriented force acting on the charged particles inside the object (Giancolly 2000, p. 802; Sivukhin 2008f), it is clear that the relation between the Poynting vector of the absorbed EM field and the vector quantity  $\Delta V[1,2]$  is becoming inevitable. The change of the sign of the vector quantity  $\Delta V[1,2]$ , observed at the beginnings of the heating and cooling periods of the modulation cycles (Fig.3b), gives the indication that the force of pressure of the EM field, acting on the charged particles in the artifact in the vicinity of the gauging surface, is also changed at that time moments. But this situation is equivalent to the conditions of observations of hysteresis loops in ferromagnetic or ferroelectric materials (Sivukhin 2008e), when the change of the direction of the external field (constant in magnitude) results in the opposite direction of the force, acting on the particles. So, to obtain the hysteresis loop of TSE, arising from the square-wave energy modulation, it is sufficient to present

the dependence  $\Delta T[1,2]$  on time as shown in Fig.2, but obtained for the whole *modulation* period, and to invert the current time at the beginning of the cooling period of the modulation cycle. The resulting TSE hysteresis loop is presented in Fig.5. Here, it is explicitly taken into account that the quantity  $\Delta T[1,2]$  is measured relative to the reference function, and so it is automatically equal to zero for the above indicated reference points at the end of each modulation cycle. In Fig.5, the experimental points for the last 35 minutes of the first modulation cycle, presented in Fig.1, are shown as squares (between the arrows 1 and 2) for the current time  $t$ . Then the data points for the heating period of the next modulation cycle, with the total duration of 35 minutes of the current time  $t$ , are presented with dots (between the arrows 2 and 3). And at last, the data points for the first 70 minutes of the cooling period of the next cycle (between the arrows 3 and 1) are presented with rhombi. Here, as the X-variable we plot the function  $(406-t)$ , measured in minutes. As it follows from Fig.5, for the time instant, indicated by arrow 1, the difference between the data points, belonging to two different modulation cycles, is absolutely negligible in comparison with the magnitude of the hysteresis loop. The obtained form of the hysteresis loop characterizes the energy loss of the artifact during the modulation cycle. The TSE loop is similar to the hysteresis loop of a hard ferromagnetic material, which can be obtained in strong magnetic fields.

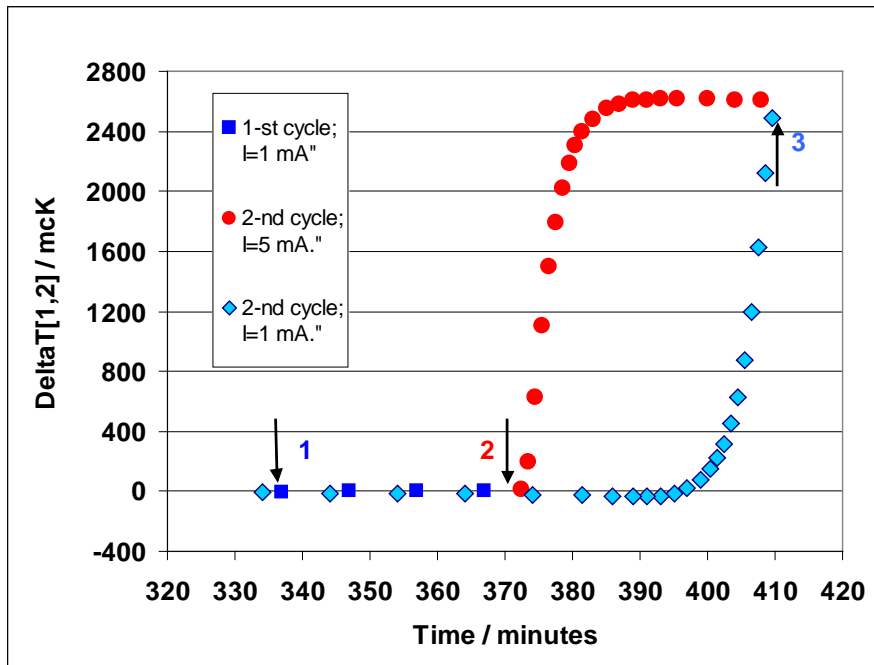


**Fig.5.** The thermal hysteresis loop for the quantity  $\Delta T[1,2]$  that corresponds to the temperature records of Figs. 1 and 2. The heating period of the cycle is shown by dots, while the cooling part is presented by rhombi and squares. (See text for other details).

Now, using the Weyl idea how to check the symmetry in time of an arbitrary physical process (Feynman, Leighton & Sands 1964), we shall show that the evolution process of the thermal surface energy is also irreversible in time. To prove this, we can assume that the modulation of the current in the PRT is produced by a rechargeable battery, an ideal electronic switch, and the energy, stored in the battery, is continuously measured and recorded. Then, in accordance with the Weyl criteria, if the backward play of the record of a process reveals some contradictions with some well-established laws of Physics, then this process is irreversible in time. In our case, for the backward play of the record, we shall observe that for the square wave current modulation in the PRT, under the fixed external conditions, we observe a purely periodic process, presented by the stationary loop of Fig.5, and the energy of the battery is increased only as result of the cooling of the thermal reservoir. But such process is in obvious contradiction with the Clausius-Plank formulation of the second law of Thermodynamics (Sivukhin 2008b), which presents the result of the analysis of a huge number of experimental facts and has no exemptions. So, we are coming to the conclusion that *the process of the build-up and disappearance of the surface thermal energy, presented by the experimental plots of Figs. 1, 2 and 5, is definitely irreversible in time.* This is in agreement with the general, fundamental statement of (Giancolly 2000, p. 528), which says that it has been found (experimentally) that all real processes are irreversible in time. Thus, *the thermal evolution process, characterized by the quantity  $\Delta T[1,2]$  is irreversible in time and has also no symmetry in space,* as it follows from the plots of Figs. 2 and 5.

Now we shall describe another important, fundamental result of this study, which is closely related to the above mentioned properties of TSE. Experimental dependencies in the following figures show the effect of non-linearity of the artifact material on the evolution process of the thermal surface energy, characterized by the quantity  $\Delta T[1,2]$ . In Fig.6, we show the build-up of the quantity  $\Delta T[1,2]$ , observed in the steel GB during the first 13 minutes after the increase of the modulation current to 5mA. The main differences relative to the experiment of Fig.2 are the following. First, the separations between the adapters of the PRT and thermistors were increased from 10mm to 13.5mm, in order to study the effect of the distance of the heat source from the gauging surface on the TSE amplitude. Second, two additional, auxiliary heat sources (constant resistors) were located inside the Dewar at the same distances from the GB and were positioned symmetrically relative to the gauging surfaces of the block. When one of them was switched on, the dc current through this resistor produced a controlled, desired temperature difference between the locations of the thermistors R6 and R3. Thus in this experiment, *the difference in the induced temperature*

*variations*, recorded by the channels 1 and 2, was measured when there was a systematic temperature difference on the artifact surface at the locations of the thermistors (belonging to channels 1 and 2). The temperature difference between the channels,  $T[1,2]$ , shown as an additional parameter in Fig. 6, was measured as a mean value of the temperature difference between the two thermistors, observed for the last 30 minutes of the cooling period of the modulation cycle. We note here that the measurements of Fig.6 were performed both for negative and positive values of the quantity  $T[1,2]$ , and the range of the variation of this parameter was between  $-2.46\text{mK}$  and  $61.06\text{mK}$ . It is clearly demonstrated by the presented plots of Fig.6 that, first, the difference between the temperature variations  $\Delta T[1,2]$ , recorded synchronously by the two channels, depends also on the temperature bias  $T[1,2]$ , produced by an auxiliary heat source. It means that thermal systems are nonlinear ones. Second, the difference in the quantities  $\Delta T[1,2]$ , corresponding to different temperature biases  $T[1,2]$ , is gradually increasing with time interval, elapsed after the increase of the PRT modulation current. And this means that we observe a complicated evolution process, when the parameters of the thermal hysteresis loop, shown in Fig.5, are slightly changing from one cycle to the other as a result of the presence of the auxiliary heat source.

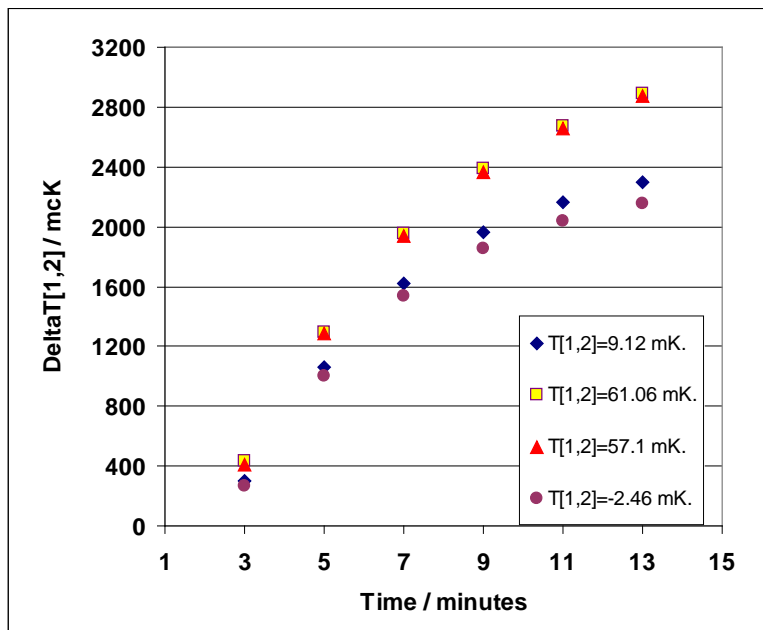


**Fig.6.** The records of the build-up in time of the thermal surface energy in a steel GB during the first 13 minutes of the heating period of the modulation cycle that were obtained for the temperature differences between the channels  $T[1,2]$  equal to:  $2.46\text{mK}$  (dots),  $9.12\text{mK}$  (rhombi),  $57.1\text{mK}$  (triangles) and  $61.06\text{mK}$  (squares). These dependences show that the principle of superposition is not valid for thermal fields. (See text for other details).



The resolution of the modulation technique is very high and gives an opportunity to measure precisely the difference between the TSE values, corresponding to the increase of the temperature difference  $T[1,2]$  from 57.1mK to 61.1mK. From Fig.6 it follows that for all of the time intervals in the range from 3 to 13 minutes, the systematic differences in  $\Delta T[1,2]$ , resulting from the change of the temperature bias  $T[1,2]$  by only 4mK, are well above the noise level corresponding to the 2 minutes time averaging procedure, which is used in the studies of Fig.6.

As the quantity  $\Delta T[1,2]$  corresponds to the difference in the temperature variations in the channels 1 and 2 that are induced by the increase of the current in the PRT, and as the magnitude of the induced temperature variations is affected by the presence of the second, auxiliary heat source, it means that *the superposition principle of thermal perturbations is not valid in case of TSE.*

This experiment also gives an indication that the excessive flux of energy to the elementary volumes of the artifact in the vicinity of the gauging surface (shown in Figs. 2a and 2b) is related, probably, to the reflection of the guided EM field inside the artifact from the nearest gauging surface, so that the EM field of the external source, irradiating that surface, helps to support the reflected field, increasing (as a result of non-linear properties of the material) the propagation length of this reflected field.

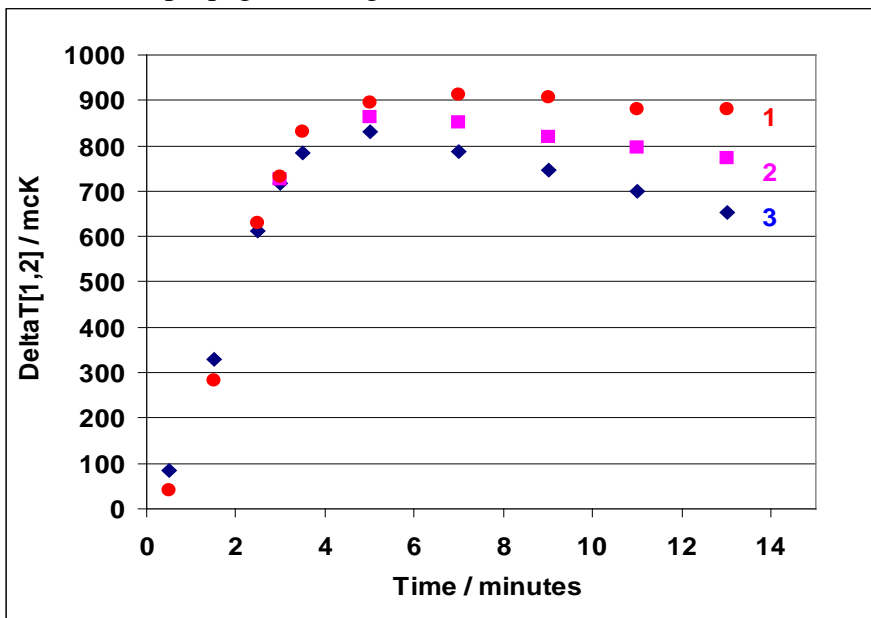


**Fig.7.** The records of the thermal evolution process, characterized by the quantity  $\Delta T[1,2]$ , that were obtained for the tungsten carbide block for the temperature differences between the channels  $T[1,2]$ , which were produced by an external heat source and which were equal to -1.72mK (dots); -7.2mK (squares) and -12mK (rhombi).

Another very important result of the studies is demonstrated by the plots of Fig.7. Here, we present the variations of the quantity  $\Delta T[1,2]$  as a function of time also in the presence of an additional heat source, but these measurements were performed on a 100-mm tungsten carbide (TC) block, where the process of the build-up of the TSE is found to be about 3 times faster than in the steel GB. In this case we observe some new features of the evolution process. As it follows from Fig.7 (in contrast to the plot of Fig.6), the negative value of the quantity  $T[1,2]$  can modify the type of the TSE dependence on time for the TC block even during the first 13 minutes of the heating period of the modulation cycle: the quantity  $\Delta T[1,2]$  as a function of time passes through its maximum value. The fundamental feature of the process is that the time interval, which is needed for the realization of the maximum value of  $\Delta T[1,2]$ , and the TSE magnitude, both are simultaneously reduced with the increase of the negative value of the temperature difference  $T[1,2]$  between the locations of the thermistors. *Thus, an additional heat source in irreversible way modifies the thermal evolution process, produced by the purely periodically modulated energy source.* From this we can infer that only the EM radiation from the Sun, which reaches the Earth's surface, is sufficient for the realization of the continuous processes of thermal evolution in material objects on the Earth's surface. This is a result of the unpredictable, irreversible character of the Earth's rotation (Guinot 2011) and the existence of the thermal surface energy, which is characterized simultaneously by the hysteresis effect and by the invalidity of the superposition principle for any two sources of EM radiation.

When analyzing the presented dependences of Fig.7 in the time interval between 0.5-1.5 minutes, we find a fascinating result. The auxiliary heat source, producing a stationary energy flux in the direction of the thermistor R6, is increasing the quantity  $\Delta T[1,2]$ , i.e. is increasing the energy flux in the direction of the R6 thermistor, which is stimulated by the increase of the PRT modulation current. For this time interval we have, practically, a pure running wave of the propagating energy, as the reflection from the gauging surface is quite small, because the product of the indicated time interval and the mean velocity of the energy propagation is smaller than the distance from the PRT to the gauging surface. Thus, it is demonstrated experimentally that when the energy reflection from the boundaries is negligible, *the thermal response of the absorption medium to the propagation of the EM field (that is induced by the modulated energy source) is significantly increased by the presence of the energy flux in the same direction that is created in advance by the auxiliary energy source.* This effect can be called as a thermal hysteresis effect for the running heat waves in the medium with absorption. As it follows from Fig.7, this effect can be of primary importance. For example, for the time interval  $t$  after the increase of

the modulation current of 0.5 minute, the quantity  $\Delta T[1,2]$ , corresponding to the temperature bias  $T[1,2]$  of -17.2mK between the positions of the thermistors, exceeds by more than 2 times the quantity  $\Delta T[1,2]$ , corresponding to the bias of -1.2mK. At longer time intervals  $t$ , when the energy, propagating with the group velocity (Loudon, Allen & Nelson 1997, p.1081), reaches the zone of the R6 thermistor after the reflection from the gauging surface, the effect changes the sign, as it is clearly demonstrated by the dependences 1-3 in Fig.7 at the current time value of 13 minutes. The effect at the artifact boundary (gauging surface) is much stronger: the magnitude of the effect at  $t=13$  minutes exceeds the magnitude of the effect in the bulk material at  $t=0.5$  minute by more than 5 times. The non-linear properties of the medium can be always observed at the boundary (see second harmonic generation in quantum electronics), and the material boundaries are usually the standard source of energy irregularities. We consider that the validity of this theoretical prediction of A. Einstein (1905) is confirmed experimentally by the present studies. But as the similar effect for the quantity  $\Delta T[1,2]$  is observed in the bulk material, the extension of the concept of the surface energy to much more general case, given by D. V Sivukhin (2008a), is of primary importance and is also confirmed by the presented studies.

### 3. Conclusions and discussions

Before starting discussions, it is worth noting that the main parameter, affecting the indications of the resistance thermometers that were used in these studies, is the energy of EM field, which is produced by the motion of the charged particles in the measured artifact. The part of this energy, absorbed in the thermometer, is effectively converted into the random motion of the particles that affects the recorded resistance value of the thermometer. This statement is the consequence of the Poynting's theorem of Electrodynamics, which says that the rate of change of the electromagnetic energy plus the total rate of doing work by the fields over the charged particles within the volume of a material artifact is equal to the flux of the Poynting vector,  $\mathbf{S}$ , entering the volume of the artifact through its boundary surface (Jackson 1999 p. 260). So, the vector  $\mathbf{S}$  describes the energy - flux density of EM field ((Jackson 1999), or the energy current density (Loudon, Allen & Nelson 1997). For the dielectric material with arbitrary level of losses, the continuity equation for the total energy density for the coupled EM field and dielectric lattice, under the approximations made in (Loudon, Allen & Nelson 1997), can be presented in the form (see eq.(2.17) in the latter reference):

$$\frac{\partial}{\partial t} W + m\Gamma \left(\frac{\partial}{\partial t} s\right)^2 = -\nabla \mathbf{S} \quad \dots(1).$$

Here,  $W$  presents the total energy density, which contains the kinetic and potential energy densities of the of the optic vibrational mode in addition to EM field energy density;  $s$  is the relative spatial displacement field of two ions in the primitive unit cell;  $m$  is the reduced mass of two ions in the primitive unit cell, and  $\Gamma$  is the damping rate of the optical mode.

The rate of energy variations, described by the first two terms, can be detected by the resistance thermometer and corresponds to the experimentally measured thermal velocity at the specified point of the material artifact. Indeed, the reading of the thermometer depends on the power absorbed from the EM field, and in accordance with the Poynting's theorem, the power, radiated by the material artifact, is defined by the total rate of the energy loss of the EM field and of the energy loss of the optical mode, representing the oriented motion of the charged particles that is directly coupled with the EM field (Loudon, Allen & Nelson 1997) . And the second term in eq.(1) describes the rate of loss of the energy of the optical mode, which is converted into heat as a result of intrinsic non-linearity of the system. And the thermometers are traditionally used to characterize the random part of the energy of the material artifacts. So, if in Fig.3b we see that the quantity  $\Delta V[1,2]$  is not equal to zero during a short interval of time after the change of the PRT current, it means that there is an additional energy flux (positive or negative) to the elementary volumes  $(dx)(dy)(dz)$  in the vicinity of the thermometer R6 relative to the elementary volumes in the vicinity of the thermometer R3. As in accordance with eq.(1) these energy fluxes arrive inside these volumes through their boundary surfaces as a result of the energy current density, described by the vector  $\mathbf{S}$ . As these fluxes are different, it means that the Poynting vectors, corresponding to the guided EM field at two different locations inside the artifact, which are located symmetrically relative to the energy source, are also different at that periods of time. From this we infer that the basic assumption of the Fourier thermal conductivity theory (TCT), which is borrowed from the steady-state experiments and which states that the thermal energy flux is defined by the temperature gradient (Sivukhin 2008c), is not valid for any period of the heat transfer process! Especially, it is not true for the "transients" of the propagation process of the thermal energy. As it follows from Fig.3a, the maximum energy fluxes to the unit volumes inside the artifact, which are located symmetrically but in the opposite directions relative to the energy source, differ by ~40%, the energy flux to the vicinity of the R6 sensor being larger. But the temperature in the system was adjusted in such a way that the temperature of the artifact surface close to R6 sensor was already somewhat higher than the temperature close to R3 sensor before the increase of the modulation current. During the whole heating period of the modulation cycle, the temperature difference  $\Delta T[1,2]$  continues to increase, and the

quasi steady-state condition at the end of the heating period is characterized by the equal thermal fluxes (see Fig.3a), and this equality is observed for the largest temperature difference  $\Delta T[1,2]$  of about  $\sim 2.5\text{mK}$ . Meanwhile, at the end of the cooling period of the modulation cycle, the energy fluxes to the unit volumes in the vicinities of both sensors are, practically, equal, but the temperature difference between the PRT and the thermistor R6 is somewhat smaller (by  $\sim 0.5\text{mK}$ ) than the temperature difference between the PRT and the thermistor R3. From this it follows that *TCT can give reasonable agreement with the temperature measurements of moderate precision only for the steady-state periods of the heat transfer process*, but TCT predictions about the initial periods of the heat transfer are not reliable.

The other very important observation, which is necessary for the interpretation of the presented experimental studies, follows from the solid-state physics (Kittel 2005). It is known that for a charged particle inside the solid-state the conserved quantity is the total momentum, which consists of the kinetic momentum of the translational motion of the charged particle, and the potential momentum of the EM field (Kittel 2005, p. 661). As pointed out by C. Kittel, this requirement on the total momentum leads to the proper equation of the Lorentz force, acting on the charged particle (Kittel 2005, p. 663).

This is in agreement with the conservation laws of electrodynamics (Griffiths 19997; Jackson 1999). The momentum of EM field, stored in the volume of a material artifact, is defined by the integral over this volume of the electromagnetic momentum density  $\mathbf{G}_{EM}$ , which (in accordance with eq. (6.118) in (Jackson 1999) ) is given by:

$$\mathbf{G}_{EM} = \mathbf{S} / c^2 \quad \dots (2),$$

where  $c$  is the velocity of light in vacuum. The continuity equation of Electrodynamics (see eq. (6.122) in (Jackson 1999) ) states that the first derivative in time of the total momentum of the field-particle system inside the artifact, consisting of the EM momentum and the momentum of the charged particles, which is varied in time by the EM (Lorentz) force acting on the particles (see eq.(6.114) in (Jackson 1999)), is defined by the flow through the boundary surface inside the artifact volume of the EM momentum current density, which is given by the Maxwell stress tensor (see eq.(6.120) in (Jackson 1999)). Thus, from the fundamentals of Electrodynamics and the Solid-state Physics it follows that the “conserved” quantities of the field-particle system inside material artifact can be the total momentum and the total energy densities of the system. So, in agreement with the presented experimental studies, the temperature, as a physical parameter characterizing the internal energy of a macroscopic elementary volume inside the artifact, should inevitably include the energy of EM field in addition to the energy of the particles. And the experimental result of the

primary importance of these studies is that the internal energy includes both: the random type of the motion of the field-particle system (with the mean values of the linear momentum and angular momentum equal to zero) and the systematic part, which describes the oriented propagation of the thermal energy and momentum that are defined by the Poynting vector of the external EM field. In this respect our experiments present some confirmation of the important theoretical studies of R. Loudon, L. Allen and D. F. Nelson (1997), dealing with the propagation of the energy and momentum through an absorbing dielectric with an arbitrary level of losses. The essential features of the theory (Loudon, Allen and Nelson 1997) are the inclusion of contributions from EM field and from dielectric medium to the total energy density  $W$  and taking into account the Röntgen term in the current density in Maxwell equations that changes the relation between the magnetic field  $\mathbf{H}$  and magnetic induction  $\mathbf{B}$  (by introducing the term, depending on the polarization of the medium  $\mathbf{P}$  that is induced by electrical field). Similarly, the total momentum density, which is called wave-momentum density, consists of the EM field momentum and the pseudomomentum density, and is found to be  $[\mathbf{D} \times \mathbf{B}]$  plus a dispersive term, accounting for the thermal losses in the system (see eq.(3.25) in (Loudon, Allen and Nelson 1997)). Here,  $\mathbf{D}$  denotes the vector of the electrical displacement of the medium.

The main results in this study are illustrated by the one-dimensional case of a plain transverse EM wave, propagating in z-direction of dielectric material with arbitrary losses. The intensity of the EM field in z-direction is assumed to fall exponentially with the characteristic length  $L$ , as a result of the gradual conversion of the energy of the optical mode into heat (see eq.(3.11) in (Loudon, Allen and Nelson 1997, p. 1074)). Under these approximations, the cycled-averaged value of the total-energy current density in the z-direction  $\langle \mathbf{S}_z \rangle$  (the only nonzero component of the Poynting vector) is related to the cycle-averaged energy density  $\langle W \rangle$  (see Eq. (2.19) in (Loudon, Allen and Nelson 1997, p. 1073)) by a simple relation (4.16):

$$\langle \mathbf{S}_z \rangle = \mathbf{v}_e \langle W \rangle \quad \dots (3),$$

where  $\mathbf{v}_e$  is the velocity vector of the energy propagation in the material. Both parameters, the velocity of the energy propagation  $\mathbf{v}_e$  and the energy density  $W$ , can be precisely determined with high accuracy from our experimental data, corresponding to one dimensional case. For example, the estimations of the energy density are quite reliable, as: 1) the thermometers cover the whole width of the artifact; 2) they are calibrated to measure the temperature of the surface at a specified point of a particular material (Titov et al. 2005, p. 587904-04); 3) temperature variations in the vertical direction of the blocks are quite negligible; 4) thermal capacity of the materials are well known; 5) temperature measurements are performed synchronously at several locations with the high resolution in time. And the other parameter in

eq.(3) - the velocity of energy propagation  $v_e$  can be accurately determined from the plots of Fig.2a. The magnitude of the velocity vector is quite small, and for the steel GB is found to be of the order of 10 mm/min.

Under the approximations adopted in (Loudon, Allen and Nelson 1997), we can have a reliable estimation of the wave momentum density  $\mathbf{G}$  of the field-particle system. For the plane TEM field propagating in z-direction, it follows from this study that the cycle averaged value of the corresponding component of wave momentum density  $\langle G_z \rangle$  is defined by the total-energy density  $\langle W \rangle$ , also averaged over the oscillation cycle, and the value of the phase velocity  $v_p$ :

$$\langle G_z \rangle = \langle W \rangle / v_p \quad \dots (4).$$

The phase velocity values for steel and tungsten carbide blocks are well known, as the refraction index of the medium  $\eta$  and the extinction coefficient of the medium  $\kappa$  can be precisely measured by optical ellipsometry. For steel gauge blocks, the refractive index  $\eta$  is 2.2 and  $\kappa=3.4$  for the wavelength of 0.63

et al. 2001). These values are in agreement with very accurate measurements of the phase change at optical reflection by optical interferometry (Titov, Malinovsky & Massone 2003).

It also follows from ((Loudon, Allen and Nelson 1997, p. 1079) that in one dimensional case, the cycle-averaged rate of the energy conversion into heat  $\langle R_H \rangle$  can be presented in a form:

$$\langle R_H \rangle = v_e \langle W \rangle / L \quad \dots (5).$$

Under the same conditions, it follows from eq.(4.23) in (Loudon, Allen and Nelson 1997, p. 1079) that the cycled averaged z-component  $\langle F_z \rangle$  of the total force density  $\langle \mathbf{F}_t \rangle$ , which consists of the Lorentz force density (acting on the particles) and of the time derivative of the EM field momentum density, can be described by the expression:

$$\langle F_z \rangle = [(1 + \eta^2 + \kappa^2) / (2\eta^2)] (\langle R_H \rangle / v_p) \quad \dots (6).$$

This expression explicitly states that the mean force, acting on the unit volume inside the artifact, is defined by the cycled averaged rate of the energy conversion into heat  $\langle R_H \rangle$  and the parameters of the medium  $\eta$  and  $\kappa$ .

As it follows from (Loudon, Allen and Nelson 1997), the expressions (3-6) are valid for the monochromatic wave as well as for the wave, described by a short Gaussian pulse. And in both of these cases, the intensity of the EM field falls exponentially along the direction of the energy propagation. So, the existence of the thermal surface energy, first observed for the case, when an external heat source irradiates by thermal EM field one of the gauging surfaces of a 900mm steel GB (see Fig.8 in (Titov et al. 2005)), looks quite natural from the theory, resulting in equation (5). Indeed, from the general physical considerations (as the consequence of conservations of energy and momentum) it is natural to expect that the EM

□; for tungsten

field, propagating in the absorbing material, will have the maximum amplitude at the boundary, which is irradiated by the external energy source, as the Poynting vector inside the medium, in accordance with (Loudon, Allen and Nelson 1997), is falling exponentially along the propagation distance. So, in accordance with eq.(5), the rate of the conversion of the total-energy energy density into heat is to fall exponentially with the increase of the separation from the boundary, and the appearance of the thermal surface energy (that is in agreement with the definition of TSE, given in (Sivukhin 2008a) is inevitable.

On the other hand, in (Titov & Malinovsky 2011) it has been shown experimentally that the heat energy in a homogeneous, well thermally isolated material artifact can propagate large distances with very small damping (see Fig.8 in (Titov & Malinovsky 2011, p. 68)). It means that when in the presented experiments, the gauge block surface is irradiated by an external heat source, then, in accordance with the basics of Electrodynamics (Loudon, Allen and Nelson 1997), the wave momentum density  $\mathbf{G}$  of a coupled field-particle system should be detectable at any point of a 100mm block. But if the total momentum, consisting of the momentum of the charged particles and the momentum of the EM field, is not equal to zero, then, in accordance with the wave momentum continuity equation (3.23) in (Loudon, Allen and Nelson 1997, p.1076), some part of the total momentum will be inevitably reflected from the boundary, and the reflected total-energy and momentum densities will produce an additional energy flux to the unit volumes of the artifact in the vicinity of the boundary. From this we can conclude that the general theoretical observation of A. Einstein (1905) about the importance of taking into account the surface energy has been confirmed experimentally for a particular case of the thermal surface energy, when the main features of the process can be understood from the concepts and theorems of Electrodynamics. We are to note here that the largest deviations from equilibrium conditions are usually observed close to the boundaries and the observation of the TSE in accordance with A. Einstein (1905) prediction is much easier than the observations of the TSE in the bulk material in accordance with the concept of TSE, presented by D. V. Sivukhin (2008a). It is also worth noting that under the approximation of a plane TEM field, adopted in section IV of (Loudon, Allen and Nelson 1997), the z-component of the wave momentum can be described by eq.(4), and the rate of the energy conversion into heat by eq.(5), here. And the parameters  $\langle W \rangle$  and L corresponding to the wave, reflected from the gauging surface and propagating in the z-direction away from the boundary, can be determined quite accurately from the experimental plots of Figs. 2a, 2b, 6 and 7. Indeed, these plots are obtained from the differential energy measurements, performed synchronously at the specified time intervals and



for several distances from the gauging surface by averaging the results of the measurements in x,y-directions. From these plots it follows, for example, that the energy density  $\langle W \rangle$  is changing continuously in time and in space and represent one of the parameters of the evolution process, which is irreversible in time, has no symmetry in space and has easily detectable hysteresis features. The other parameters of this process are the total-energy current density  $\mathbf{S}$ , the wave momentum density  $\mathbf{G}$  and the total force density  $\mathbf{F}_t$  that are described approximately by the equations (3), (4) and (6). *These parameters describe the new properties of the artifact medium that are acquired as a result of interaction with the external energy and momentum sources of the environment.* The non-zero parameters of the evolution process  $\mathbf{S}$ ,  $\mathbf{G}$  and  $\mathbf{F}_t$  do not simply exist under the thermal equilibrium conditions. So, we have an evolution process, when the properties of a material artifact, representing the part of the interacting system are changed in response to the changing external conditions. Such process in literature is sometimes called as a “self-ordering” process, but it is much more appropriate to call this process as *synthesis*, as in this meaning it was first introduced into philosophy by the XVIII century German philosophers H. M. Chalybäus and J. G. Fichte and is commonly used nowadays in Chemistry. Indeed, in the thermal evolution process, the material artifact changes its properties and characteristics as a result of the “consumption” from the environment the material quantities of momentum and energy, delivered to the object by the external EM field.

The irreversible in time change of the properties of the material objects, subjected to hysteresis evolution process, are well known in many fields of Natural Science. The most spectacular and well studied example is the Earth (Guinot 2011). As a result of interaction with material objects of the Universe and evolution processes in the planet, the pole of the planet is in continuous motion with respect to the Earth's crust, with well-detected daily unpredictable wobble of the pole, with the presence of the quasi-periodic components with the durations 1.0 and 1.2 years and with the pole secular drift along the meridian  $80^\circ$  (Guinot 2011). When these pole variations are combined with magnitude variations of the angular velocity of the Earth's rotation that have “random”, quasi-periodic and secular components, which resulted in the accumulated effect of -34 seconds during 50 years relative to the time scale of atomic standards (Guinot 2011), we can immediately conclude from the presented temperature studies that all thermal evolution processes on the Earth are unpredictable and irreversible in time as a result of a continuously changing amount of the energy, received from the Sun by the objects on the Earth's surface due to irregularities of the Earth's rotation. From this we can conclude that the discovery of the thermal surface energy has a fundamental impact on Electrodynamics in general. Indeed, as

predicted by N. Ramsey (1963) theoretically and first shown experimentally by P. Kusch, the process of interaction of the EM field with the quantum system is always nonlinear (Ramsey 1963). So, from the equation (V, 55) in (Ramsey 1963) it follows immediately that if in the “thermal” range of energies of EM field the symmetry in time is not observed (or in other words, the process of interaction of the field with matter is irreversible), then the lack of symmetry in time is inevitable in Electrodynamics for the whole range of energies of the EM field.

It should be specially emphasized that the irreversible character of the material processes was known in Astronomy for many years, so that the concept of the arrow of time was introduced in 1927 by British astronomer Arthur Eddington. According to A. Eddington, the distinguished direction of the time - the basic physical quantity - can be determined by the study of organizations of material objects in the Universe.

On the other hand, the lack of symmetry in space, which is typical for thermal evolution processes and is clearly demonstrated by the plots of Figs. 1 and 2, is not also something unique, but is well known from the experimental studies of the hysteresis effects in ferromagnetic (Sivukhin 2008d) and ferroelectric (Sivukhin 2008e) materials. As pointed out in (Sivukhin 2008e), the important distinguishing feature of the hysteresis effect in these materials is the lack of symmetry in space that arises as a consequence of the presence of the external field (magnetic or electric). It has been demonstrated experimentally that when an external electric field is applied to a ferroelectric sample ( $\text{BaTiO}_3$ , for example), there starts a gradual process of the growth of the domains with the favorable direction of the polarization (when the polarization vector coincides with the direction of the applied field) at the expense of the domains with the unfavorable polarization. This effect as a function of time can be studied in detail by the observations of the domains in a polarized light (Sivukhin 2008e, p. 167). And this is one of the experimental proofs of the asymmetry in space in case of the hysteresis effect. The other proof is the *change of the properties* of the material as a result of the presence of the evolution process in the presence of the oriented force. For example, it has been proved experimentally that in  $\text{BaTiO}_3$  crystal, the positive edge of the domain is etched faster by the acid than the negative edge (Sivukhin 2008e, p.167). The experimentally observed lack of symmetry in time and in space, typical for the hysteresis effects in ferromagnetic and ferroelectric materials (Sivukhin 2008d, 2008e) as well as for the presented studies of the thermal evolution process, are in agreement with the much more general violations of symmetries (Sakharov 1967; Sakharov 1972) in Physics, which have been first predicted and explained theoretically by the prominent Russian physicist A. D. Sakharov in case of the physics of elementary particles (Sakharov 1972).

It also follows from equations (5) and (6), presented here, that the propagating energy in the medium with absorption always produces the force on the unit volume of the medium, which is changing continuously in time and in space, and inevitably produces a complicated pattern of stresses and deformations in the medium. And it is known from many fields of Natural science that stresses can change dramatically the properties of the materials. For example, it follows from material science that metals and plastics, subjected to periodically changing level of stresses and deformations, are becoming brittle after some time and dismantle to small pieces under the application of the force, orders of magnitude smaller that they were able to withstand at the beginning of the test process. And this is one of the spectacular demonstrations of the violation of time “symmetry” in the real processes in Nature. On the other hand, it is an indication of the important role of the EM interactions in the evolution processes, as in the indicated test process there is no any transfer of particles between the parts of the test system and all the interactions are realized through EM fields.

The process of the gradual changes of the properties of the material standards in the presence of stresses and deformations (which can be called also as the synthesis process) is known in many fields where accurate measurements of properties of macroscopic objects are possible. For example, in precise interferometric length measurements, the measured length of the material standard (gauge block) does depend on the level of deformations, existing between the gauge block and the reference plate. (Titov et al. 2001; Titov, Malinovsky & Masssone 2003). So, the length of the gauge block is defined in the wrung condition to the reference plate. Using modern fringe pattern analyzing interferometers it is possible to study the process of the build-up these deformations in time and in space (Titov, Malinovsky & Masssone 2003, p. 46). High-precision length measurements should be realized in this case after the time interval, when the variations of the measured length in time are becoming comparable or less than the uncertainty of the length measurement procedure. The method, resulting in the dramatic decrease of the wringing deformations on the result of the interferometric measurement, has been also developed (Titov, Malinovsky & Masssone 2001, p. 39; Titov et al. 2001, p. 16).

In comparison with the optical interferometry, the temperature measurements offer much easier way for the detection of the evolution process. In the water triple point (WTP) cell, the basic temperature standard used for the definition of the temperature unit (Kelvin), the record of the evolution process in time (see Fig.8 in ((Titov, Malinovsky & Masssone 2001, p. 37)) can be realized by a single standard platinum resistance thermometer (SPRT) and a high-precision bridge. In comparison with the steel artifact, the WTP cell is characterized by a much more sophisticated

evolution process, as the temperature, recorded by SPRT, is only about  $150\mu\text{K}$  below the phase transitions ice-water-vapour. And this temperature is dependent on the presence of the field of gravity (or thermometer immersion depth effect), on the isotopic composition of water surrounding the thermometric well of the cell, on the presence of chemical impurities, on the presence of stresses in the ice mantle and on the prehistory of the WTP cell, such as the way how the ice mantle was created from the super-cooled water or what is the time interval passed after the creation of the ice mantle. As in WTP cells or Gallium standards the resolution of temperature measurements of  $\sim 1\mu\text{K}$  can be achieved (see Figs 7 and 8b in ((Titov, Malinovsky & Masssone 2001)), the enumerated dependences can be studied with quite high signal-to-noise ratio. For example the part of the evolution process, presented by the plot of Fig.8a in (Titov, Malinovsky & Masssone 2001), is associated with the gradual changes of the isotopic composition and chemical impurities in a thin water layer between the mantle and the thermometric well of the cell in a newly created ice mantle, but after the relaxation of mechanical stresses. (The study of the other effects will be presented elsewhere.)

### **3.1. Comparison with some philosophical doctrines**

The main results of the presented studies are in agreement with the tenets of many philosophies, starting with the philosophies of Ancient India and Ancient Greece and finishing with dialectic materialism. But what is interesting, the presented experiments give some additional information so that we can check the exactness of the statements of different philosophy doctrines. Here, we are to remind that the fundamental triad (thesis-antithesis-synthesis) was stated by H. M. Chalybäus as comprising three dialectical stages of development: a thesis, giving rise to its reaction, an antithesis, which contradicts or negates the thesis, and the tension between the two being resolved by means of a synthesis. Although this model is often named after Hegel, Hegel has never used that specific formulation. The XVIII century German philosopher J. G. Fichte greatly elaborated on the synthesis model, which was later incorporated into dialectic materialism. Usually, the Fichtean Dialectics are considered to be based upon four concepts:

1. Everything is transient.
2. Everything is composed of contradictions.
3. Gradual changes lead to turning points when quantitative change leads to qualitative change.
4. Change is helical (spiral), as a manifestation of negation of the negation.

The first two of the indicated concepts of dialectic existed in the philosophy of Heraclitus of Ephesus, who is famous for his observation of continuous, ever-present changes in the universe, as stated in the famous saying (“panta rhei”): "All entities move and nothing remains still. No man ever steps in the same river twice". Heraclitus clearly emphasized the importance of the *unity of opposites*, stating that *all existing entities are characterized by pairs of contrary properties*. His famous cryptic utterance is "all entities come to be in accordance with this *Logos*" (i.e. “the account which governs everything”). As Diogenes explains the fundamentals of the Heraclitus philosophy:” All things come into being by the conflict of opposites, and the whole ensemble of things flows like a stream”. Heraclitus basic idea of the tension between two opposing forces can be also traced in the much older Hindu Philosophy, where the two complements, "*purusha*" and the "*prakriti*", bring everything into existence, following the *Dharma* (the Universal Law of Nature).

Another quite original, fundamental principle can be found in the Ancient Indian *Jain* philosophy. As per *Jainism*, the truth or the reality is perceived differently from different points of view, and that no single point of view can represent the complete truth. The fundamental Jain doctrine of *Anekantavada* states that all entities have infinite modes of existence and qualities, and, consequently, these entities cannot be completely perceived in all their aspects and manifestations by human beings as a result of the inherent, intrinsic limitations of the mankind.

The fundamental Jainism doctrine is clearly in agreement with the presented experimental studies. Indeed, for the TSE the principle of superposition is shown to be not valid, so the thermal systems are basically nonlinear systems. As a result of the TSE existence, all energy sources of the Universe are in nonlinear interaction with each other through a hysteresis type of the evolution process, and the linear momentum of EM field from each source, irradiating the surface of the artifact, has to be taken into account when finding the solution for the guided field inside the artifact. As the interaction of the EM field with an ensemble of charged particles is basically different from the interaction of the EM field with a single particle (Dicke 1954, p. 99). As shown by R. Dicke (1954, p.105), the ensemble of atoms, interacting with the common field, is characterized by the properties, which has no symmetry in space. As emphasized in (Dicke 1954, p. 105) the “coherence is limited to a particular direction only”, and the whole process of interaction depends crucially on the specific features of the excitation of the ensemble (Dicke 1954, p. 99; Stroud et al. 1972, p. 1098). The process of the emission of coherent spontaneous radiation is time irreversible (Dicke 1954; Stroud et al. 1972) and it stops when the total dipole moment of the ensemble becomes equal to zero (Stroud et al. 1972, pp. 1099-1100), but

when some energy of the initial excitation is trapped in the system (Stroud et al. 1972; Cummings & Dorri 1982). As it follows from eqs. (10)-(11) in (Stroud et al. 1972), the number of influence parameters, which are necessary for the description of the ensemble of atoms, is becoming absolutely huge: all the separations between the atoms, the mutual orientations of dipoles of each pair of atoms, and the initial excitation parameters of each atom are to be taken into account. All these main predictions of theoretical analysis of (Dicke 1954; Stroud et al. 1972) has been confirmed by our experiments. Only the number of influence parameters in the experiment is much larger, as besides the enumerated parameters the information about the forms, materials, energy spectrum and emission diagrams of each object will further enlarge this number, even in the simplest case of the experiments in a free space. For the real experiments performed on the Earth's surface, the number of influence parameters should be considered as infinite, as the Solar energy (which is always detected by precise thermoeters) is propagating through turbulent atmosphere, and the number of macroscopic parameters is infinite in this case of turbulence (Sivukhin 2008a). The enormous number of influence parameters results in the huge number of modes of existence of a thermal system, so that in confirmation of the fundamentals of Jain philosophy, no human being can perceive adequately, in all aspects the thermal evolution process.

We can also infer that the well-known triad (thesis-antithesis-synthesis) is basically in agreement with the presented experiments, but the evolution process by German philosophers is understood as a simple mechanical process, when thesis as a first stage of the evolution process is substituted later by the second phase (anti-thesis), and the tension between them is resolved later by synthesis. All these concepts can be found in the experiment, but there is one crucial distinction. Thesis and anti-thesis are the opposite properties of a particular material object, and these properties coexist simultaneously without mixing in the object as a result of conservation laws of momentum and energy, which are preserved in each elementary absorption-emission process with huge accuracy. But for periods of time of about 1 hour, these conservation laws are not any more valid, as the result of the exchange of momentum and energy with the infinite material objects of the Universe. So, the synthesis process undergoes continuously and is the fundamental property of the Universe or "this logos" as it was called by the great Heraclitus of Ephesus. For example, the presented in Fig.1 the process of thermal evolution can be described as helical, in agreement with Fichtean dialectics. Naturally, in our experiments, the span of the spiral is defined by the magnitude of the periodic modulation in the PRT current, and only the variations of each modulation cycle of this spiral and its deformations in time are caused by the irreversible processes in the

Universe and, in particular, by the irreversible character of energy transfer from the Sun to a fixed point Earth's surface. In this respect our studies and conclusions are in agreement with the discovery of Charles Darwin and Alfred Russel Wallace "On the Tendencies of Species to form Varieties, and by Perpetuation of Varieties and Species by Natural Means of Selection on the"( 1858), when the result of the long-term influence of the surrounding Nature on the evolution of living species (organisms) has been unambiguously established. What is demonstrated here is that the similar synthesis process with the continuous creation of the new properties of the material object does occur in non-living material objects. Naturally, in case of living objects the evolution process due to interaction with the outside Nature is much more spectacular and can be observed even with "naked eye", but requires usually long observation periods. Meanwhile, in the presented experiments on thermal synthesis, as a result of the use of the sophisticated measurement procedure, the change of the properties of the material artifact, described by the approximate relations (2)-(6), can be clearly detected within 1 hour.

In conclusion we are to note, that the presented studies are in agreement with the standard practice of laser cooling of the beams of neutral atoms (Wineland, Drullinger & Walls 1978). If the frequency of the laser light is lower (red-shifted) than the frequency of a stationary atom, then the atomic beam is cooled, and the force acting on the atoms is in the opposite direction to the velocity of atoms in the beam (in agreement with the requirement of conservation of impulse of the system). If the laser light is blue-shifted, then the force is in the opposite direction and the energy of the atomic ensemble is increased. Similar effects are demonstrated here by the plots of Fig.3.

At last, it is pertinent to make some remarks about the concepts of thermodynamic equilibrium and thermodynamic temperature. It is known (Sivukhin 2008a; Sivukhin 2008b) that the thermodynamic relations are based on the idea of the adiabatic enclosure, so that the states of the system inside such enclosure can be connected by a quasi-static process, for which it is assumed that the number of parameters (necessary for the description of this process) is equal to the necessary number of parameters under the thermal equilibrium conditions (Sivukhin 2008a). But as a result of the existence of the thermal surface energy (reported here), the thermal evolution process is becoming irreversible in time, *the number of influence parameters in TSE, describing the input of momentum to the system, is increased dramatically, so that the very concept of thermodynamic temperature is to be ruled out in principle* (Sivukhin 2008a). In other words, the idea of adiabatic enclosure is always in contradiction of the infinitely slow quasi-static process, as the physical meaning of the TSE is that energy and momentum

are always propagating inside any type of the enclosure, if its outer surface is irradiated by the thermal EM field. So, the adiabatic enclosure is the approximation of theoretical physics, which is in evident contradiction with the experiment (the concept of the arrow of time, following from numerous astronomical observations). In this respect, the mathematical theory of thermal conductivity by J. Fourier is much closer to reality, as, at least, it predicts the irreversible type of thermal processes. But as this theory does not contain any considerations about the continuity of the wave momentum of the material artifact and does not take into account the deformations of the lattice and mass transfer as a result of the EM field pressure, the validity of this theory is, probably, restricted to quite slow, stationary (asymptotic) phases of the heat transfer processes in a solid state.

### **Acknowledgements**

The authors gratefully acknowledge financial support of our studies at INMETRO by the National Research Council (CNPq) of Brazil. The technical and moral support of our studies by the staff of INMETRO is highly appreciated. The authors are grateful to the staff of the Physical department of the Yeditepe University (Turkey) for useful discussions and the offered possibility to present our results at the International Conference “Chaos-2013”.

### **References:**

- Dicke, RH 1954, “Coherence in Spontaneous Radiation Processes”, *Phys. Rev.*, vol. 93, no. 1, pp. 99-110.
- Stroud, CR, Eberly, JH, Lama, WL & Mandel L 1972, “Superradiant Effects in Systems of Two-Level Atoms”, *Phys. Rev. A*, vol. 5, no. 3, pp. 1094-1104.
- Einstein A 1905 “Investigations on the Theory of the Brownian Motion”, *Annalen der Physik*, vol.17, no.3, pp.549-566.
- Sivukhin DV 2008a, “*Thermodynamics*”, 4th edn, vol.2, pp.44-71 in General Course of Physics, Physmatlit, Moscow.
- Sivukhin DV 2008b, “*Thermodynamics*”, 4th edn, vol.2, pp. 85-110 in General Course of Physics, Physmatlit, Moscow.
- Sivukhin DV 2008c, “*Thermodynamics*”, 4th edn, vol.2, pp. 162-182 in General Course of Physics, Physmatlit, Moscow.
- Sivukhin DV 2008d, “*Electricity*”, 4th edn, vol.3, pp. 293-317 in General Course of Physics, Physmatlit, Moscow.
- Sivukhin DV 2008e, “*Electricity*”, 4th edn, vol.3, pp. 159-172 in General Course of Physics, Physmatlit, Moscow.
- Sivukhin DV 2008f, “*Electricity*”, 4th edn, vol.3, pp. 613-621 in General Course of Physics, Physmatlit, Moscow.
- Einstein A 1903, “A Theory of the Foundations of Thermodynamics”, *Annalen der Physik*, vol. 11, no. 2, pp.170-187.



- Titov, A & Malinovsky, I 2005, “Nanometrology and high-precision temperature measurements under varying in time temperature conditions”, in Recent Developments in Traceable Dimensional Measurements III: *Proc. SPIE*, vol. 5879, eds. J. E. Decker & Gwo-Sheng Peng, pp. 587902-01 – 587902-11, SPIE, Bellingham, WA.
- Titov, A & Malinovsky, I 2011 “New techniques and advances in high-precision temperature measurements of material artefacts”, *Can. J. of Scientific and Industrial Research*, vol.2, no.2, pp. 59-81.
- Titov, A, Malinovsky, I, Erin, M, Belaidi, H, & Franca, RS 2005, ”Precise certification of the temperature measuring system of the original Kősters interferometer and ways of its improvement”, in Recent Developments in Traceable Dimensional Measurements III: *Proc. SPIE*, vol. 5879, eds. J. E. Decker & Gwo-Sheng Peng, pp. 587904-01 – 587904-11, SPIE, Bellingham, WA.
- Titov, A, Malinovsky, I & Masssone, CA 2001, “Scientific basis for traceable dimensional measurements in a nanometer range: methods and concepts”, in Recent Developments in Traceable Dimensional Measurements: *Proc. SPIE*, vol. 4401, eds. J. E. Decker & N. Brown, pp. 33-43, SPIE, Bellingham, WA.
- Einstein, A 1917, “ Zur Quantentheorie der Strahlung”, *Physikalische Zeitschrift*, vol. 18, no.1, pp. 47-62.
- Griffiths, DJ 1999, “Introduction to Electrodynamics”, Prentice Hall, 3d edn, pp.346-355, Upper Saddle River, NJ.
- Giancolly, DG 2000, “Physics for Scientists and Engineers”, Prentice Hall, 4th edn, p.802 ; p.528, Upper Saddle River, NJ.
- Feynman, RP, R. B. Leighton, RB & Sands, M 1964, “The Feynman Lectures on Physics”, Addison-Wesley, vol. 1, Ch.52, pp.1-12.
- Guinot, B 2011, “Solar time, legal time, time in use”, *Metrologia*, vol. 48, no.2, pp. S181-S185 (2011).
- Loudon, R, Allen, L & Nelson, DF 1997, “Propagation of electromagnetic energy and momentum through an absorbing dielectric”, *Phys. Rev., E*, vol. 55, no.1, pp. 1071-1085.
- Jackson, JD 1999, ”Classical Electrodynamics”, J. Willey and Sons, 3d edn, Hoboken, NJ, pp.259-262.
- Kittel, C 2005, “Introduction to Solid State Physics”, J. Willey and Sons, 8th edn, Hoboken, NJ, pp. 661-665.
- Titov, A, Malinovsky, I, Masssone, CA, Garcia, GA, Kleinke MU & Dotto, MER 2001, ”Deformations of a gauging surface under wringing conditions”, in Recent Developments in Traceable Dimensional Measurements: *Proc. SPIE*, vol. 4401, eds. J. E. Decker & N. Brown, pp. 11-22, SPIE, Bellingham, WA.

- Titov, A, Malinovsky, I & Massone, CA 2003, “Wringing deformation effects in basic length measurements by optical interferometry”, in *Recent Developments in Traceable Dimensional Measurements II: Proc. SPIE*, vol. 5190, eds. J.E.Decker & N.Brown, pp. 43-53, SPIE, Bellingham, WA.
- Ramsey, NF 1963, “Molecular beams”, Clarendon Press, Oxford, pp. 115-144.
- Sakharov, AD 1967, “Violation of CP Symmetry, C-Asymmetry and Baryon Asymmetry of the Universe”, *JETP Lett.*, vol.5, no.1 pp.24-27.
- Sakharov, AD 1972, "Topological structure of elementary particles and CPT asymmetry" in "*Problems in theoretical physics*", dedicated to the memory of I.E. Tamm: Nauka, Moscow, pp.243-247.
- Cummings, FW & Dorri, A 1982, “Exact Solution for spontaneous emission in the presence of N atoms”, *Phys. Rev. A*, vol.28, no. 4, pp.2282-2285.
- Darwin, Ch & Wallace, AR 1858, “On the Tendencies of Species to Form Varieties, and the Perpetuation of Varieties and Species by Natural Means of Selection”, *Journal of the Proceedings of Linnean Society of London, Zoology 3*, vol. 3, no.9, pp. 46-50.
- Wineland, D, Drullinger, R & Walls, F 1978, “Radiation Pressure Cooling of Bound Resonant Absorbers,” *Phys. Rev. Letters*, vol. 40, no.11, pp. 1639–1642.